Biophysical Journal, Volume *112*

Supplemental Information

Unbiased High-Precision Cell Mechanical Measurements with Microconstrictions

Janina R. Lange, Claus Metzner, Sebastian Richter, Werner Schneider, Monika Spermann, Thorsten Kolb, Graeme Whyte, and Ben Fabry

Supplementary Information

Unbiased high-precision cell mechanical measurements with microconstrictions

Janina R. Lange[1], Claus Metzner[1], Sebastian Richter[1], Werner Schneider[1], Monika Spermann[1], Thorsten Kolb[2], Graeme Whyte[3] and Ben Fabry[1]

[1]*Biophysics Group, Department of Physics, Friedrich-Alexander University of Erlangen-Nuremberg, Erlangen, Germany*

[2]*Division of Molecular Genetics, German Cancer Research Center (DKFZ), Heidelberg, Germany*

[3]*IB3: Institute of Biological Chemistry, Biophysics and Bioengineering, Department of Physics, Heriot-Watt University, Edinburgh, UK*

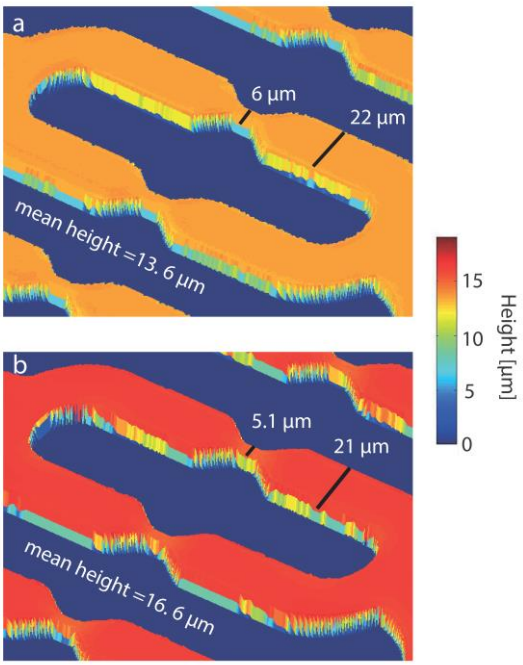

Fig. S1 Geometry of microconstriction devices:

a) "Wide constriction" and **b)** "narrow constriction" devices used for validating the histogram matching procedure (Fig. 3 of the main text). The device geometry for the constriction region is measured with a µ-surf confocal interferometric microscope (NanoFocus, Oberhausen, Germany) at a voxel resolution of 0.62 µm × 0.62 µm × 0.18 µm (length × width × height).

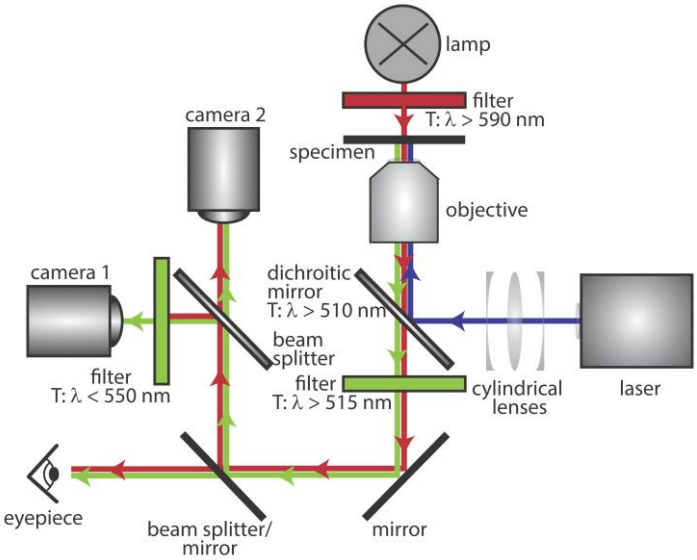

Fig. S2 Fluorescence extension of microconstriction setup:

For recording the signals from fluorescently labeled cells, a diode-pumped solid-state laser (wavelength 473 nm; VA-I-N-473, Viasho, Beijing, China) with a power of 100 mW is coupled to the epifluorescence port of the microscope (DM-IL, Leica). A combination of cylindrical lenses is used to limit the illumination field to the region of interest containing the 8 parallel constrictions. Through a series of dichroitic mirrors, excitation and emission filters and beam splitters (Thorlabs, Germany), the light for bright-field imaging (wavelength > 590 nm) is separated from the emission wavelength of GFP (~ 515-550 nm) and coupled to two separate cameras.

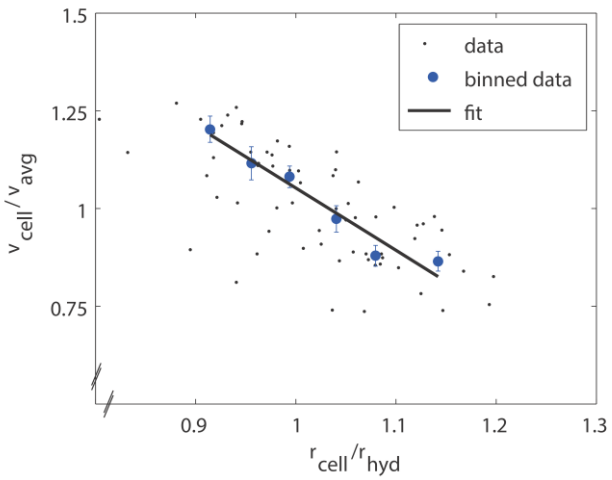

Fig. S3 Dependency of cell speed on average flow speed:

Computing the hydrodynamic pressure at each point of the channel system requires knowledge of the flow speed. We estimate the average flow speed from the speed of each cell before it enters a constriction. Because of the approximately parabolic cross-sectional flow velocity profile within a channel, smaller cells travel faster compared to larger cells for the same average flow velocity. Here, we investigate the relationship between cell velocity v_{cell} and average flow velocity v_{avg} as a function of cell radius in a rectangular channel (h = 15.5 µm, w = 20 µm). The cell culture medium is mixed with polystyrene beads of 1 µm in diameter, and their movements are tracked at the channel midsection. From the theoretical flow profile within a rectangular channel, the average flow speed can be computed as $v_{avg} = 0.48 \cdot v_{max}$, with v_{max} being the maximum speed of the beads in the middle of the channel. The graph shows the dependency of relative cell speed v_{cell} / v_{avg} on the ratio of cell radius to the hydrodynamic radius of the channel, r_{cell}/r_{hyd}. The hydrodynamic radius of the channel r_{hyd} is calculated as $r_{hyd} = h \cdot w/(h+w)$. As expected, we find that cell speed decreases with increasing cell radius. This can be approximated by a linear relationship according to $v_{cell} / v_{avg} = 2.64 - 1.59\ (r_{cell}/r_{hyd})$.

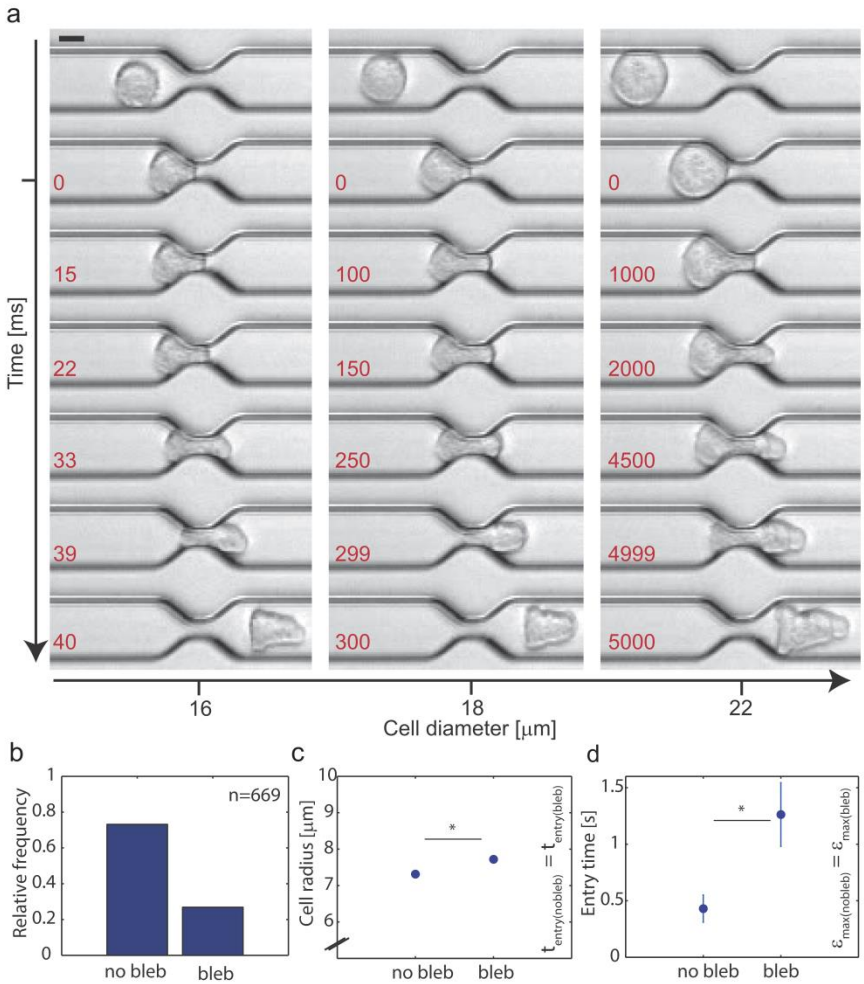

Fig. S4 Evolution of cell shape changes during transit through microconstrictions:

(a) Representative K562 leukemia cells of different sizes are imaged while passing through a 6 µm constriction at a pressure of Δp = 250 Pa. Time is shown by red numbers with zero indicating the beginning of entry. Images are contrast enhanced. Left: small cell (diameter = 16 µm) deforms in 40 ms and travels on in a bullet-like shape. Middle: medium-sized cell (diameter = 18 µm) deforms in 300 ms and travels on in a bullet-like shape. Right: large cell (diameter = 22 µm) deforms in 5000 ms. The cell forms a bleb at the leading edge, which after 2000 ms remains approximately constant in size. After exiting the channel, the cell travels on in a bullet-like shape with various membrane ruffles at the rear end and the bleb at the leading edge. Scale bar is 10 µm. **(b)** Fraction of K562 cells that form a bleb at their leading edge during transit through 5.1 µm wide microconstrictions. Approximately 25 % of all cells form a bleb (n = 669). **(c)** Dependence of bleb formation on cell size. Cells that do not form a bleb are significantly ($p<0.05$) smaller than cells forming a bleb during transit through microconstrictions (mean ± se, n=184 for both groups). For the analysis, only cell populations with the same average entry time are selected. **(d)** Dependence of bleb formation on cell entry time. Cells that do not form a bleb enter a microconstriction significantly ($p<0.05$) faster than cells that form a bleb (mean ± se, n=212 for both groups). For the analysis, only cell populations with the same average cell size are selected. After exiting the constrictions, cells reassume a round shape and withdraw the bleb completely, but the recovery time for these processes is larger than 5 min and increases with entry time or cell size (data not shown).

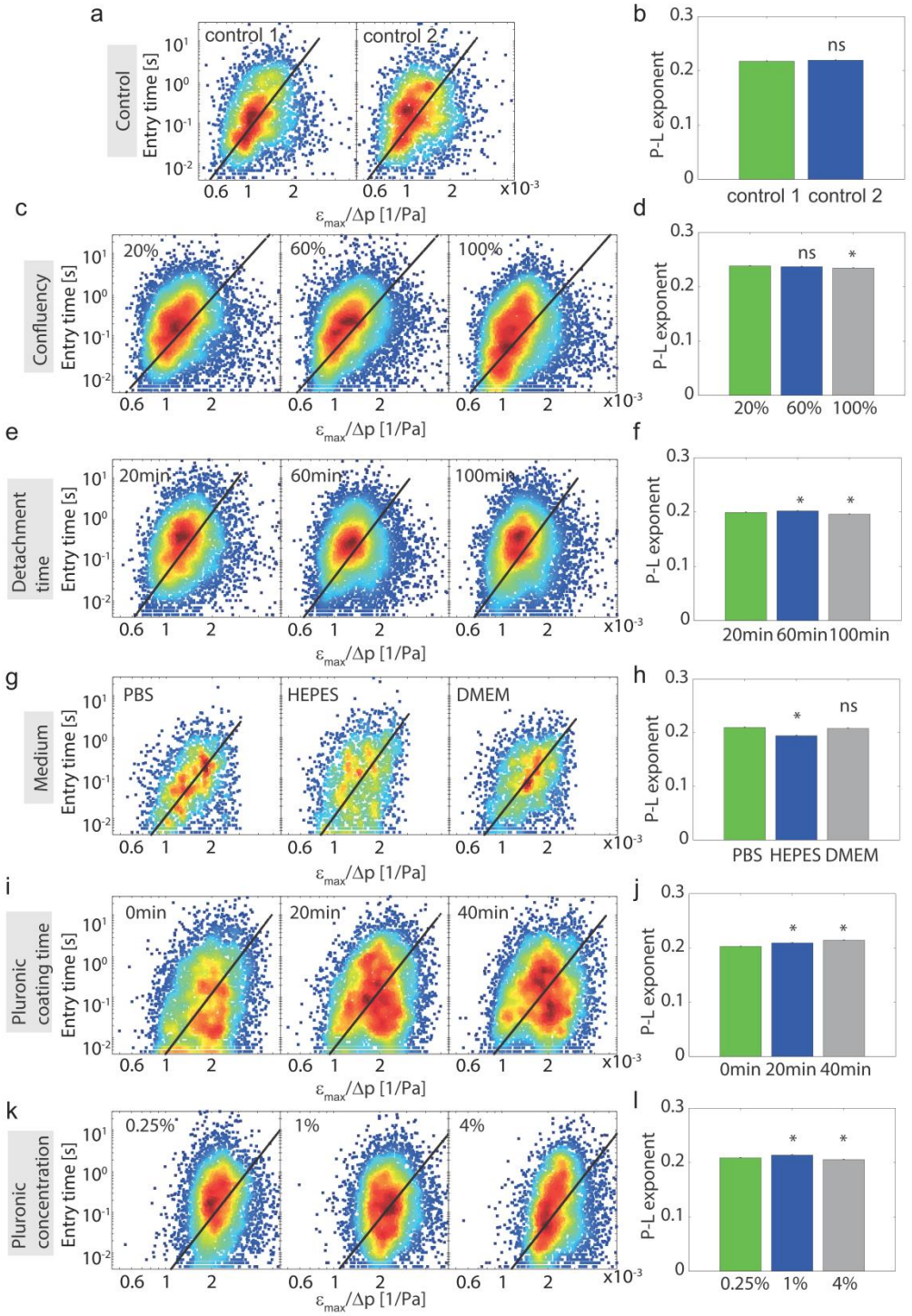

Fig. S5 Influence of culture and measurement conditions on resulting cell mechanical properties:

Scatter plots of exemplary bootstrap sample of entry time t_{entry} vs. $\varepsilon_{max}/\Delta p$ with power-law fits, and power-law exponents for different culture and measurement conditions for DLD-1 cells corresponding to Fig. 3 of the main text. **(a-b)** Control measurement: four independent measurements, performed under the same conditions, were arbitrarily split into two groups. **(c-d)** Dependence on cell culture confluency (20 %, 60 %, 100 %) prior to harvesting. **(e-f)** Dependence on detachment time of cells before measurements (20 min, 60 min, 100 min). **(g-h)** Dependence on cell suspension medium (PBS, HEPES, DMEM). **(i-j)** Dependence on pluronic coating time of the device prior to

measurements at 1 wt% pluronic concentration (0 min, 20 min, 40 min). **(k-l)** Dependence on pluronic coating concentration for a coating time of 30 min (0.25 wt%, 1 wt%, 4 wt%). n > 1200 for each plot. Error bars show one standard error of the mean. Significant differences compared to first parameter value (green bars) ($p < 0.05$) are indicated by asterisks.